POROUS POLYMER SCAFFOLDS DERIVED FROM BIORESOURCES FOR BIOMEDICAL APPLICATIONS

CRISTIAN DANIEL BOHORQUEZ-MORENO,[*] KERIM EMRE ÖKSÜZ[*] and EMINE DINÇER[**]

[*]*Sivas Cumhuriyet University, Faculty of Engineering, Department of Metallurgical and Materials Engineering, Sivas, 58140, Turkey*
[**]*Sivas Cumhuriyet University, Faculty of Health Science, Department of Nutrition and Dietetics, Sivas, 58140, Turkey*
✉ *Corresponding author: C. D. Bohorquez-Moreno, 20209253004@cumhuriyet.edu.tr*

Received September 27, 2022

The development of sustainable materials in medical treatment for the controlled release of drugs has generated interest in the field in view of the environmental and energy challenges faced during the continuous production of materials in the sector. In the present study, the potential use of sponges based on combinations of three types of starch (corn, wheat, and rice starch) with poly(vinyl alcohol) was investigated to evaluate their morphological properties, swelling ratio, *in vitro* biodegradation, antibacterial activity, hemolysis, and blood clotting index. The synthesis process is based on a cost-effective method for wide application in the medical industry, yielding sponges with a high swelling index of up to 8 times the original volume. A slight antibacterial activity was also observed when rice and corn starch were used. In addition, different morphological and physical properties were observed depending on the type of starch added to the formulation, allowing a variety of responses to treatment requirements, depending on factors such as the duration of treatment and the patient's blood characteristics in terms of clot formation or immune response.

Keywords: porous sponge, drug delivery system, *in vitro*, bio-composites, sustainable materials

INTRODUCTION

The search for materials to enhance medical treatment in a massive, economical, and sustainable way has aroused the interest of the scientific community. For instance, the use of polymeric sponges has been investigated for application in wound healing,[1–3] and adequate results of the treatment have been obtained. However, many of the materials have limitations because of their low biodegradability, cost, or complex processability. Besides, the safety of medical treatment has also become a research problem in various branches of science, with the major objective to increase the survival chances of patients, without causing further deterioration of their health. Thus, these factors have motivated the use of other strategies, such as absorbent sponges or porous scaffolds, with functionalization of their mechanically triggerable performance,[4] resulting in a promising solution in the field.[5] Notwithstanding, these materials have raised several questions related to their morphological, physical characteristics, biocompatibility, and bioactivity. Currently, the use of polymeric matrices in the design of triggerable sponges has been focused on most common polymers, such as polylactic acid, pluronic, polycaprolactone, alginates, cellulose films, and poly(vinyl alcohol) (PVA).[6–10]

Among polymeric formulations, the use of PVA has aroused interest due to its interesting biological properties, as well as its low cost and relative sustainability, but its application in various areas is often limited because of its mechanical properties.[11,12] Mixing it with other polymeric materials has been a recent matter of research aiming to increase its properties; but despite the various combinations developed, many of these are costly or environmentally compromising. Thereby, the use of more economical and bioavailable raw materials is sought as an alternative for increasing the mechanical properties of PVA.

Starch[13–15] is one such option, as it is an interesting material used in the synthesis of the next generation of delivery devices. Starch with PVA have proven to have high compatibility

owing to their solubility and interaction due to the hydroxyl groups that compose them, resulting in materials with new properties, such as biochemical stability, high mechanical performance, and low degradation.[16–18] Nevertheless, there are still challenges related to the limitations of the use of PVA-starch combinations, because of the lack of studies about the advantages and interactions among the components, especially with different combinations of starches that can affect the final microstructural, functional, and biological performance. The present study aims to analyze the morphological and physical properties, such as absorption, *in-vitro* biodegradation, antibacterial activity, hemocompatibility, and blood clotting performance of polymeric sponges based on PVA-starch combinations in order to identify their potential use in biomedical applications.

EXPERIMENTAL

Materials

Poly(vinyl alcohol) polymer (PVA-$(C_2H_4O)x$; Mw = 60,000 g/mol), formaldehyde solution 27-31% w/v (CH_2O, stabilized with about 10% methanol), hydrochloric acid (HCl) fuming 37%, and sodium carbonate (Na_2CO_3, anhydrous 99.5%, extra-pure) were purchased from Sigma-Aldrich (St. Louis, USA). Commercial wheat, corn, and rice starches were supplied from a local market in Turkey.

In the classification of the starches, the amylose content is important. The values relating to the amylose content of the starches used were as follows: corn starch – amylose content: 25%,[19] rice starch – 15%,[20] and wheat starch – 10% (waxy type).[21] The amylose content of the starches under study was in accordance with those reported in the literature related to these types of commercial starches. All the chemicals used in this study were of analytical grade and used without further purification.

Synthesis of sponges

For the synthesis of the three types of sponges, the same methodology was followed, varying the type of starch used and taking into account the fact that, in the mixtures, the Na_2CO_3, CH_2O and HCl concentrations are based on the total of the PVA matrix suspension.

PVA (10 wt%) was dispersed in distilled water (dH_2O) at 80 °C by stirring (500 rpm) for 60 min. The PVA solution was cooled below 65 °C, then 5 wt% starch was carefully added into the solution with stirring for 1 hour at 65 °C until a homogeneous aqueous solution was obtained. The PVA/Starch solution was cooled down below 55 °C. Subsequently, 1.5 wt% Na_2CO_3 was added carefully as foaming agent, continuing the agitation for 5 minutes. Then, the stirring was raised to 2000 rpm. After this, 40 wt% formaldehyde was added to the PVA-Starch-Na_2CO_3 solution, and mechanical stirring was maintained for 5 min to promote the reaction and prevent volatilization of the components. Finally, 8 wt% HCl was added to induce the formation of froth immediately. The reaction was promoted for 20 seconds, after which the stirring was stopped. In the forming process, vessels of adequate size were used, considering that the foaming process can expand up to 4 times the volume of the original suspension.

The final homogenous mixtures were poured into molds and dried at 55 °C overnight. The water-insoluble biomedical sponge was then washed several times with dH_2O to neutralize and remove the excess acid traces and starch. For this purpose, the acidity and the presence of other components in the washing solutions were checked by pH measurements and visual inspection, respectively. After the cleaning process, the samples were dried at 60 °C for 4 h. The sponges were labelled according to their composition as follows: the formulation with corn starch – SC, with wheat starch – SW, and with rice starch – SR. All experiments were performed in triplicate, each being repeated at least three times.

Morphological, physical, and functional characterization

The following characterization process was carried out for each of the PVA and starch combinations. The microstructure and surface morphology of the sponges were observed *via* a field emission scanning electron microscope (FE-SEM, Tescan Mira3 XMU, Czech Republic), at an accelerating voltage of 15–20 kV. The % porosity (average open porosity) of the sponges was measured by the liquid displacement method, which is a method proposed for the measurement of polymeric froths,[22] using displacement liquid (Decane, ($C_{10}H_{22}$), d = 0.73 g.mL^{-1}). This liquid was selected due to its low density, as it can penetrate the pores, additionally, it does not dilute, deform or cause swelling in the samples due to its low activity with the sponges. First, the sponges were sectioned into uniform parts and dried for 12 h at 55 °C to completely remove the moisture. Then, the sponges were immersed in a vessel containing decane for 2 h in a vacuum atmosphere at -675 mmHg in order to promote penetration of the decane and air displacement. The samples were carefully removed from their containers and excess decane was removed with absorbent paper. The percent porosity was measured in accordance with Equation (1):

$$P(\%) = \frac{W_i - W_d}{W_i} \quad (1)$$

where W_d is the weight of the dried sample before impregnation with decane, W_i is the weight of the impregnated sample.

Moreover, as the displacement liquid is a non-polar liquid, it acts as a sealant of the open porosity and inhibits the swelling of the samples. The bulk density of the samples was calculated by means of Archimedes' principle, with an assembly according to dimensions and displacement caused by the sponges in the aqueous medium, in compliance with Equation (2):

$$\delta = \frac{W_d * \delta_{(H_2O,@19°C)}}{W_i - W_f} \quad (2)$$

where δ is the bulk density, W_d is the weight of the dry sample before impregnation with the decane, W_i is the weight of the impregnated sample, W_f is the weight of thrust generated by the displacement caused by the sponge in the water, and $\delta(H_2O,@19°C)$ is the density of water at 19 °C.

The different functional groups of the sponges were identified by Fourier transform infrared spectroscopy (FT-IR, Bruker Alpha II). For FT-IR analysis, a regular section of approximately 1 cm of the sponges were subtracted and evaluated in an ATR sampling analysis device.

In-vitro *characterization*

The swelling ratio of the sponges was evaluated in the following way: first, regular parts of the sponges were extracted and immersed in 2 mL of phosphate buffer solution (PBS) with a pH of 7.4 at 37 °C. The sponges were maintained immersed for different time periods from 1 to 8 weeks. After each immersion period, a sample was taken out to determine the swelling ratio. Each sample was carefully removed from the study container and the excess fluid was wiped off with filter paper. The swelling rate was calculated according to Equation (3):

$$S_i = \frac{W_s - W_d}{W_d} \quad (3)$$

where W_s is the weight of the sample after the immersion, W_d is the weight of the dry sponge before immersion, and S_i is the swelling index. In addition, the study environment was carefully renewed each week to avoid phosphate precipitation and change of ionic levels in the containers.

The degradation of the sponges was evaluated by *in vitro* degradation tests by incubation in PBS solution at 37 °C (pH 7.4). The samples were evaluated for the same 8-week period, taking out one sample each week for measurement. After each evaluation period, the samples were carefully washed to remove excess trace elements and dried at 55 °C for 24 h. Then, the degradation rate was calculated according to Equation (4):

$$D_i\ (\%) = \frac{W_0 - W_d}{W_0} x100 \quad (4)$$

where W_0 is the weight of the sample before degradation and W_d is the weight of the washed and dried sample after the degradation period; D_i is the degradation rate.

Evaluation of antibacterial activity

A modified disk-diffusion method was used to evaluate the antibacterial activity of different sponge samples. For the assay, the sponges were shaped to the size of 1 cm x 1 cm, and sterilized by UV irradiation for 5 minutes. Two indicator microorganisms, *Staphylococcus aureus* ATCC 29213 and *Escherichia coli* ATCC 25922, were chosen to represent gram-positive and gram-negative microorganisms, respectively. An antibiotic disc of Cefamezin (CFZ, 30 µg) was used as positive control. The process was as follows: 1% (v/v) active cultures of indicator microorganisms were transferred into the nutrient broth and incubated at 37 °C for 16 h, bacterial density was adjusted according to McFarland standard No. 0.5, using the same medium. Then, 1 mL was taken and transferred to nutrient plates (agar-plate) and was homogenized by the spread technique, after the agar surface was dried. Sterilized sponge samples were placed on the agar surface. Afterwards, the plates were incubated at 37 °C for 24 h, then the inhibition zone (mm) that emerged around the sponge samples was measured and antibacterial activity was calculated by subtracting the sample size from the zone diameter. All the assays were performed twice and the average of the results was calculated.

Evaluation of hemocompatibility

In order to evaluate hemocompatibility of the sponge samples, their hemolytic activity percentages was determined with the modified method proposed earlier.[23] Briefly, fresh blood from a healthy goat was obtained from a slaughterhouse and then stabilized with dipotassium EDTA (1.5 mg L^{-1}). To obtain healthy red blood cells (HRBCs) for the hemolysis assay as soon as the fresh blood was taken, it was centrifuged (5000 rpm for 3 min), washed 3 times and then diluted 10-fold with sterile PBS solution. Sponge samples with uniform size were placed in a sterile polypropylene test tube, then 2 mL of HRBCs was added onto the samples and kept at 37 °C for 2 h. After that, the samples were centrifuged (10.000 rpm for 1 min), supernatants were collected and the optical density values of the supernatants were recorded at 541 nm with a SPECTROstar Nano (Germany), equipped with an ultra-fast UV/vis spectrometer from BMG Labtech. A mixture of 1.6 mL of sterile distilled water with 0.4 ml of HRBCs was used as positive control. A mixture of 1.6 mL of sterile PBS with 0.4 mL of HRBCs was used as negative control. Hemolytic activity was confirmed twice for each sample and the average of two independent experiments was used to calculate the percentage of hemolytic activity. The percentage of the hemolytic activity was calculated according to Equation (5):

$$HA\ (\%) = \frac{OD_s - OD_{NC}}{OD_{PC} - OD_{NC}} x100 \quad (5)$$

where OD_S is the absorbance of the tested sample, OD_{NC} is the absorbance of the negative control and OD_{PC} is the absorbance of the positive control.

Evaluation of blood clotting property

In order to evaluate the blood clotting ability of the sponges, the blood clotting index (BCI) was determined by a method described in the literature,[24] with some modification. For the analysis, goat blood received from the slaughterhouse was placed into the anticoagulant tube and used without waiting. The study was briefly carried out as follows. Sponge samples were placed in the middle of polypropylene Petri plates and 100 µL of blood was put onto the surface of the samples. Immediately afterwards, 10 µL of 0.2M $CaCl_2$ solution was dropped onto the surface and samples were incubated at 37 °C for 20 minutes. At the end of the incubation period, 5 mL of sterile distilled water was added gently, without dispersing the clot formed. In the next step, the blood-water mixture in the plates was collected and transferred into the polypropylene test tube. After centrifugation at 10.000 rpm, supernatants were transferred to clean the tubes and incubated at 37 °C for 1 h. At the end of the incubation period, the optical density of the samples was recorded at 540 nm with a SPECTROstar Nano (Germany), equipped with an ultra-fast UV/vis spectrometer from BMG Labtech. In the optical density measurements, sterile distilled water was used as target and 5 mL of sterile distilled water with 100 µL of blood mixture (subjected to all analysis steps) was used as positive control. Blood clotting capacity was confirmed twice for each sample and the average of two independent experiments was used to calculate the BCI (%). The blood clotting index was calculated according to Equation (6):

$$BCI\ (\%) = \frac{OD_S}{OD_{Pc}} x100 \quad (6)$$

where OD_S is the absorbance of the tested sample and OD_{PC} is the absorbance of the positive control.

RESULTS AND DISCUSSION

Morphological and physical characteristics

Table 1 shows the porosity values of the sponges containing different starches in their composition. The density ($g.cm^{-3}$) and porosity (%) of the sponges are strongly related to the type of starch used, and different interactions between the components during the synthesis. According to the results, the sponges based on corn starch have the highest density and the lowest porosity; this effect is due to the difficulty of CO_2 to form large bubbles in the forming-macrostructure of the sponges. This resistance to deformation of SC-type sponges may be related to the high amylose content of corn starch and the interaction of amylose chains with PVA in the case of SC type sponges, generating low deformation of the structure because of the higher amount of H-bonds in the structure, promoting resistance in the cavities of the sponge.

On the other hand, in the case of the sponges based on rice starch, an intermediate behavior has been observed regarding density and porosity, which is related to its amylose content,[25] which promotes lower deformation, with low gas movement during the sponge formation process. The porosity and density observed in SW is associated to its lower content of amylose and the high predominance of amylopectin in its composition, increasing the resistance of the macrostructures during the synthesis. Figure 1 shows the morphology of the cross-sections of the SC-, SR- and SW-based sponges. All produced samples showed a highly microporous structure. The differences in morphology are mainly associated with the variation in the miscibility of the starches with PVA. In the formulations based on corn starch, regions with low macroporosity have been observed, with smaller pore size in these regions (yellow marks). This effect is related to the high mechanical resistance in this formulation during pore formation, which limits the free diffusion of CO_2. The same effect is evidenced in the formulations based on rice starch; though, the dense regions are smaller and lower pore density is identified in the densified regions of the material. In both cases, nodular particles (white marks) are noticed along the pore walls and some densified regions of the material. These formations are due to the high adhesive interfacial energy presented by some starch particles, despite the treatment related to the cleaning process to remove residues during synthesis. Due to their surface coalescence with the PVA-structure, these particles have promoted strong adhesion to the sponges, making their removal by continuous washing treatments unfeasible. Similar synthesis systems have been identified, where the differences in the solubility of corn and rice starches with PVA promote the existence of segregations due to the difference in viscosity of the starches and PVA,[26] which decrease the reactivity and generate residues partially incorporated in the structure.

Table 1
Density and porosity of the sponges based on different types of starch

Sponge samples	Density (g.cm^{-3})	Porosity (%)
SC	0.62	32.4
SR	0.43	46.7
SW	0.23	57.1

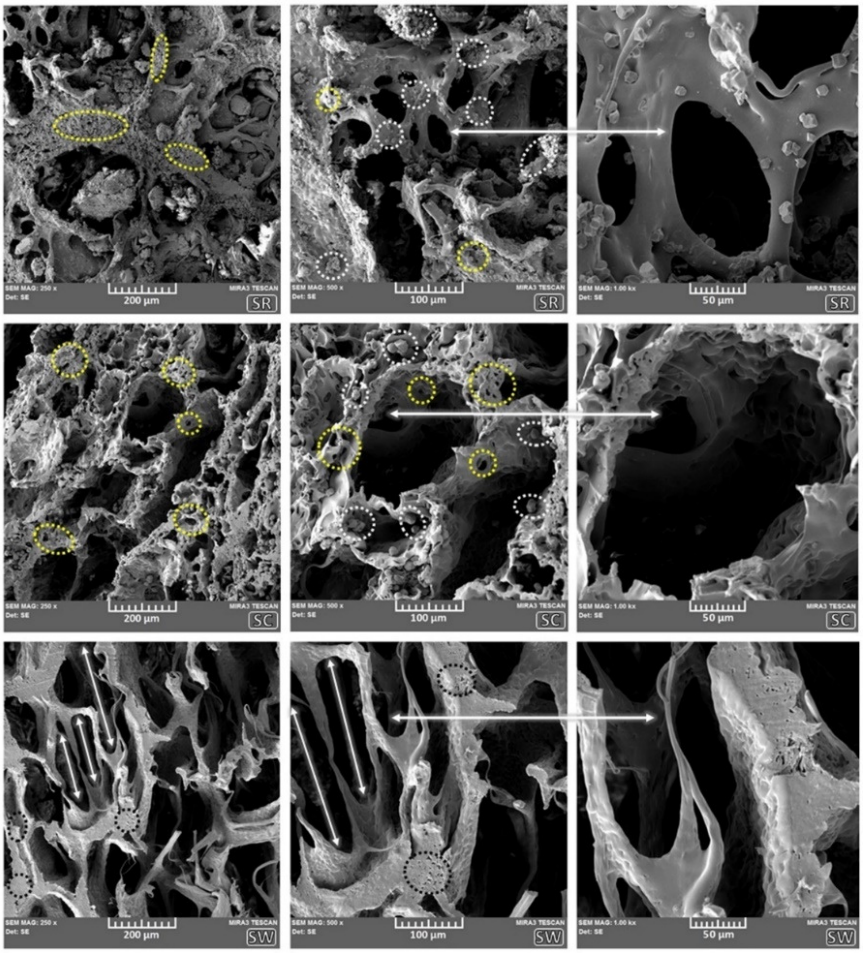

Figure 1: FE-SEM micrographs of cross-sections of SR-, SC- and SW-based sponges

In the case of formulations based on wheat starch, a homogeneous structure has been observed, with the absence of micro-nodular formations (black marks). This morphological result indicates the high miscibility of wheat starch and PVA, as observed in similar structures.[27] Moreover, other factors that have affected the miscibility differences are related to characteristics, such as grain type, amylose chain ordering and size. In this case, the lenticular morphology (white arrows), the mostly amorphous arrangement, and the existence of short chains in wheat starches tend to promote lower gelatinization temperature, compared to the corn and rice starches, characterized by long chains, polygonal shapes and high gelatinization temperatures.[28] Hence, the lower gelatinization temperature has promoted greater dissolution of the components in the case of SW, which caused no excess of partially solubilized structures, as observed for SC and SR.

Functional characteristics (FTIR)

Figure 2 shows the spectra for the SC-, SR- and SW-based sponges. In general, a wide region between 3550 cm^{-1} and 2788 cm^{-1} is observed,

related to the OH^- stretch vibrations. This functional group confirms the high interaction of the starting components in virtue of the fact that both the starch and PVA have a structure with large OH^- groups. Besides, these results evidence that the synthesis process of the sponges promoted the interaction between the components, making possible a strong interaction due to intermolecular forces of hydrogen.[15] The deformation of the band associated with the OH^- functional group has differences in intensity according to the type of starch used; as a result, rice starch and wheat starch have a more pronounced peak, compared to that of corn starch. This indicates higher amorphization of PVA due to the interaction of amylose chains with the polymer; this interaction could affect the mechanical properties of the sponges, promoting a higher degree of mechanical deformation,[14] compared to the use of corn starch, with a high intensity peak, which may be related to lower amorphization on PVA.

In the region of 3000 cm^{-1}-2780 cm^{-1}, the peak related to O–H stretching of alkyl groups,[29] and at 1700 cm^{-1}, a peak related to the presence of the stretching of C=O are observed in PVA. At 1430 cm^{-1} and 1409 cm^{-1}, peaks associated with bending vibrations and deformation of the C–H group in PVA are observed.[15,30,31] The peaks at 1393 cm^{-1} and 1246 cm^{-1} are related to bending vibrations and deformation of C–H groups in starches, respectively.[13,32,33] Only in the sponges based on corn starch and wheat starch, a peak at 1358 cm^{-1}, associated with the vibration of CH_2 groups in starches, is detected.[15,30] The peaks detected in the area of 1170 cm^{-1} and 1070 cm^{-1} are related to the vibration of C–O groups in starches, this band is characteristic for the presence of starch chains.[13,15,32,34,35] Additionally, at 1007 cm^{-1}, there is a peak related to bend-type vibrations in the glucose rings contained in the starch, these vibrations are related to the C–O–H vibrational group. Finally, at 840 cm^{-1}, there is a weak peak related to the stretching of the C–C groups in PVA. Moreover, in the region of 779 cm^{-1}-667 cm^{-1}, a weak band is observed, related to the vibration of disaccharides and polysaccharides of the starch, this weakness in the detection of the bands is related to the low content of starches in the sponges.

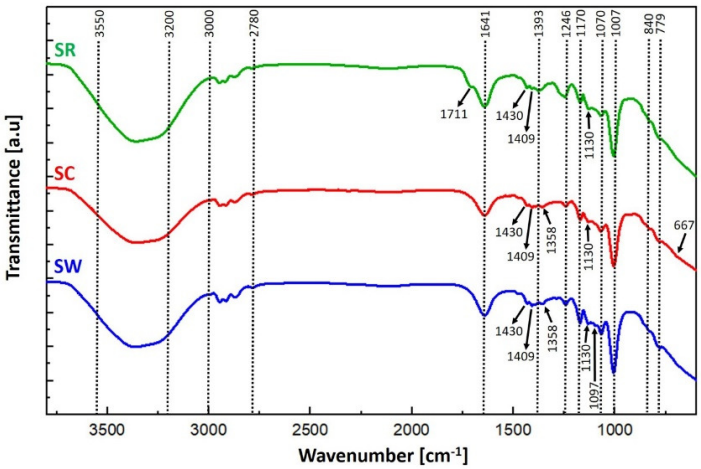

Figure 2: FT-IR spectra of SC-, SR- and SW-based sponges

In-vitro **biodegradation characteristics and swelling ratio**

Figure 3 presents the results related to the *in-vitro* biodegradation performance and swelling ratio of the sponges with different starch contents. The sponges synthesized with rice starch present higher degradation during the study period, the degradation after day 14 shows a slight increase, which can be related to the loss of polymeric chains with low adhesion. From day 21 onwards, the degradation process is accelerated due to the decrease in the degree of crosslinking between the PVA and starch chains, owing to the granulometric characteristics of rice starch, which decreased the reaction capacity and gelatinization during the synthesis. The sponges based on corn starch present an intermediate level of degradation, with an increase from day 21 to day 35. In this period, a degradation stabilization is observed, followed by a less pronounced degradation. The identified degradation behavior in the sponges is considered satisfactory,

compared with the observations regarding PVA/starch films reported in the literature, in which the degree of degradation is higher.[36–39]

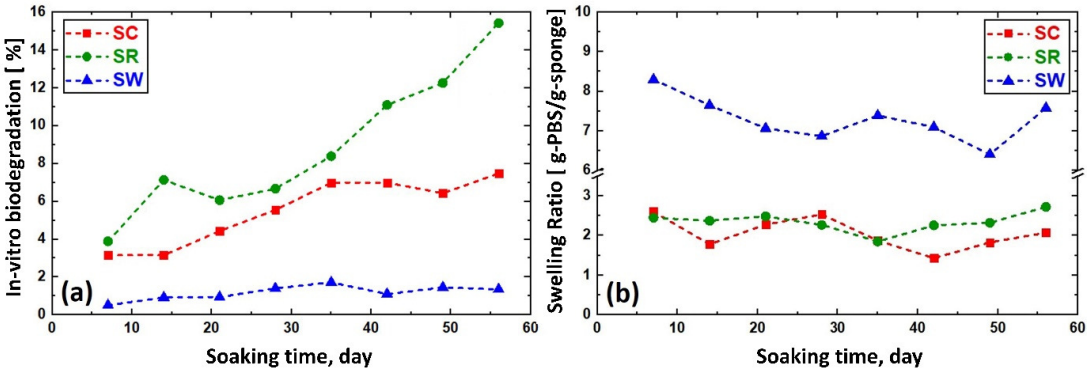

Figure 3: *In-vitro* biodegradation performance (a) and swelling ratio (b) of the sponges

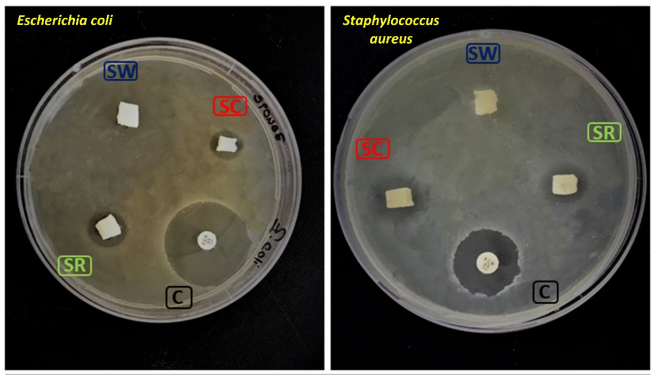

Sponge Samples	*Escherichia coli* (*E. coli*)	*Staphylococcus aureus* (*S. aureus*)
SC	4 mm	8 mm
SR	7 mm	4 mm
SW	—	—
Control (Cefazolin Sodium)	20 mm	12 mm

Figure 4: Antibacterial activity of sponges against *Escherichia coli* and *Staphylococcus aureus*

These results provide an interesting perspective for the future application of these materials as biomedical materials. On the other hand, the swelling properties of SW sponges are more pronounced compared to those of the other formulations – during the studied period, an unstable swelling feature, with a decrease in the first weeks of the test, was observed, which may be related to the specific time requirements of the sponges before equilibrium is established. The high porosity of wheat-based sponges promoted a high degree of swelling, since more regions serve as reservoirs and interact with the medium, increasing the interaction between the highly hydrophilic chains of the sponges. In the case of the sponges based on rice and corn starches, an intermediate behavior is observed, compared to SW. In SR formulations, there is high degradation over time, which is related to the interaction of the amylose chains with the medium, which increased the retention of liquid, [40] compared with the corn-based sponges. As regards SC, previous studies based on the use of corn have shown similar results of absorption in aqueous systems, as well as variations over time related to the interaction of hydroxyl bonds and degradation of the sponge in the studied period.[41]

Antibacterial activity

Figure 4 shows the antibacterial activity results for the sponges, and the measured inhibition zone diameters (mm). It is observed that SC and SR were found effective against both indicator microorganisms, and SW was found ineffective. Thus, SC is more effective against *S. aureus*, representing gram-positive bacteria, and SR is more effective against *E. coli*, representing gram-negative bacteria. As a result, the antibacterial

activity in the case of SC and SR, is associated with their low porosity, which decreases the regions available for bacterial incubation. Also, these formulations exhibit low absorption, suggesting that lower absorption, compared to SW, decreases the ideal conditions for bacterial growth.

On the other hand, the differences in bacterial sensitivity are determined by the morphological characteristics of these microorganisms[42] and their interaction with the starch chains. Therefore, the morphology of SR sponges presents a less suitable surface for the interaction of the predominant fimbrial adhesins of gram-negative bacteria, which may be related to the microstructure observed in these formulations.[43] In contrast, the SC formulation reveals that it may have beneficial effects, by decreasing the possibility of bacterial growth for gram-positive bacteria. It is related to the internal structure of the sponges, considering that the starch-PVA structure can decrease the tendency of covalent bond formation between the fimbrial subunits of gram-positive bacteria.[43,44] Besides, the nodular structures in SR and SC can serve as protection mechanisms against bacterial growth, due to the highly activated exposed area of these regions, which diminished the activity of the bacterial membranes during their proliferation. In the case of the SW formulation, the observed homogeneous morphology without granulations provides the conditions for its insignificant antibacterial activity, since homogeneous structures offer a continuous medium that promotes the growth of biofilms commonly associated with the type of bacteria observed.[45,46]

Evaluation of hemocompatibility and anti-thrombogenic properties

Figure 5 (c-d) shows the obtained hemolysis (%) and blood coagulation index clotting values for the PVA-starch sponges. The SR formulation presents a low hemolysis value, compared to the SC and SW ones, especially the latter, for which a high value is obtained. The high hemolytic capacity of the SW formulation is related to its high absorption capacity, which influences the tonicity of the medium and generates a hypotonic condition for erythrocytes. Thus, the cells undergo swelling and burst because of the difference of pressure, generating the hemolytic state.

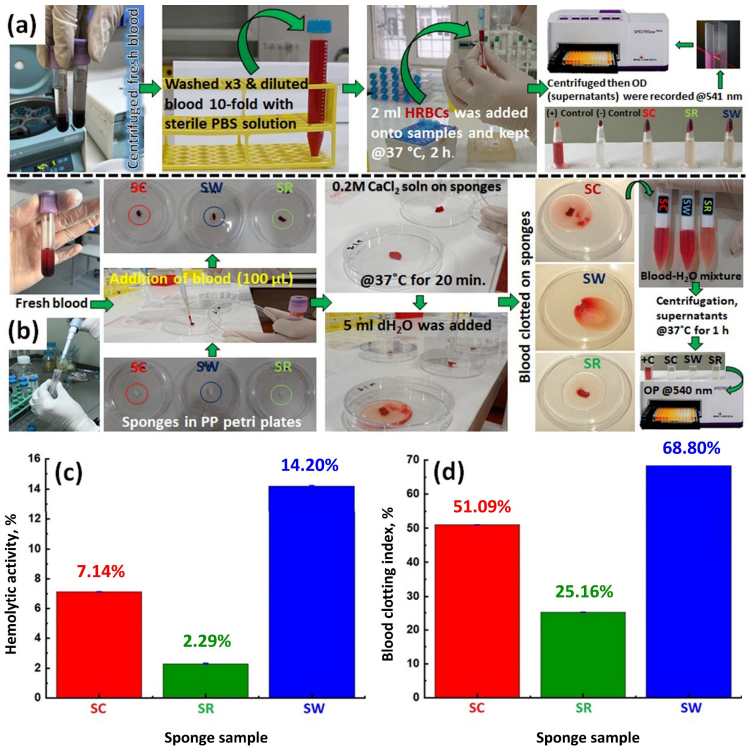

Figure 5: Schematic representation of test steps: (a) *in-vitro* hemolysis and (b) blood clotting assay of sponge samples with fresh blood (photos from our laboratory); (c) Hemolytic activity (%) and (d) blood clotting index (%) of the sponge samples

This effect is counteracted in low absorption froths that prevent the creation of a hypotonic state for the cells, like the formulations based on SR and SC. According to ASTM standards (ASTM F756-00),[47] SC is considered hemolytic, which limits the possibility of its use in healthcare. Hence, only SR sponges are considered slightly hemolytic and suitable for use in healthcare.

In order to understand the blood clotting index (BCI) results, it is important to note that the blood clotting assay determines the anti-thrombogenic properties of various biomaterials in contact with whole blood, based on the amount of free hemoglobin in the medium. Therefore, high blood clotting index means less clotting on the biomaterial surface and, as the BCI increases, materials are considered anti-thrombogenic. The creation of clots based on the coagulation reactions triggered by the action of calcium ion is an important element of the test. The activation of coagulation is strongly related to the activity of calcium in the process, since it serves in the binding process between different complexes and in activating some factors in the process. Thus, the BCI results for the SW and SC sponges are related to their high absorption capacity towards calcium ions. In the SW formulation, its high porosity also increases the absorption of calcium ions. In the case of the SR sponge, its tendency toward clot formation is related to the fact that the chains of this type of structure have a lower degree of freedom for calcium ionic absorption.

CONCLUSION

The present research has studied the effect of different types of starch on the properties of sponges intended for application in the biomedical sector. High porosity and low density have been observed in wheat starch formulations, with a low tendency to promote clots and no beneficial antibacterial activity. In the case of the formulations based on corn and rice starches, intermediate density was observed, with an adequate degree of porosity and absorption for biomedical applications. Also, these formulations offer a lower degree of degradation, with antibacterial activity and interesting hemolytic properties, in spite of a slight tendency toward clot formation. These properties make the sponges suitable for short-term treatments. As a result, the development of such sponges may be promising considering their potential applicability in the biomedical area, as their properties may respond to the current necessities in the field, with additional benefits of low cost and environmental friendliness.

REFERENCES

[1] P. Li, L. Cao, F. Sang, B. Zhang, Z. Meng *et al*., *Biomater. Adv*., **134**, 112698 (2022), https://doi.org/10.1016/j.msec.2022.112698

[2] B. Verbraeken, E. Lavrysen, R. Aboukais and T. Menovsky, *World Neurosurg*., **156**, 53 (2021), https://doi.org/10.1016/j.wneu.2021.09.007

[3] Y. Fan, Q. Lu, W. Liang, Y. Wang, Y. Zhou *et al*., *Eur. Polym. J*., **157**, 110619 https://doi.org/10.1016/j.eurpolymj.2021.110619

[4] X. Zhao, J. Kim, C. A. Cezar, N. Huebsch, K. Lee *et al*., *Proc. Natl. Acad. Sci. U.S.A*., **108**, 67 (2011), https://doi.org/10.1073/pnas.1007862108

[5] K. Shi, R. Aviles-Espinosa, E. Rendon-Morales, L. Woodbine, J. P. Salvage *et al*., *ACS Biomater. Sci. Eng*., **7**, 180 (2021), https://doi.org/10.1021/acsbiomaterials.0c01608

[6] K. Shi, R. Aviles-Espinosa, E. Rendon-Morales, L. Woodbine, M. Maniruzzaman *et al*., *Colloids Surfaces B Biointerf*., **192**, 111068 (2020), https://doi.org/10.1016/j.colsurfb.2020.111068

[7] N. Y. Elmehbad, N. A. Mohamed, N. A. Abd El-Ghany and M. M. Abdel-Aziz, *Cellulose Chem. Technol*., **56**, 983 (2022), https://doi.org/10.35812/CelluloseChemTechnol.2022.56.88

[8] M. Abrisham, M. Noroozi, M. Panahi-Sarmad, M. Arjmand, V. Goodarzi *et al*., *Eur. Polym. J*., **131**, 109701 (2020), https://doi.org/10.1016/j.eurpolymj.2020.109701

[9] X. Fan, M. Li, Q. Yang, G. Wan, Y. Li *et al*., *Mater. Sci. Eng. C*, **118**, 111408 (2021), https://doi.org/10.1016/j.msec.2020.111408

[10] A. Z. K. Lo, S. K. Lukman, C.-H. Lai, N. M. Zain and S. Saidin, *Cellulose Chem. Technol*., **55**, 539 (2021), https://doi.org/10.35812/CelluloseChemTechnol.2021.55.48

[11] N. Jain, V. K. Singh and S. Chauhan, *J. Mech. Behav. Mater*., **26**, 213 (2017), https://doi.org/10.1515/jmbm-2017-0027

[12] T. S. Gaaz, A. B. Sulong, M. N. Akhtar, A. A. H. Kadhum, A. B. Mohamad *et al*., *Molecules*, **20**, 22833 (2015), https://doi.org/10.3390/molecules201219884

[13] W. Razzaq and A. Javaid, *J. Fac. Eng. Technol*., **22**, 27 (2015), https://doi.org/http://journals.pu.edu.pk/journals/index.php/jfet/article/viewFile/483/306

[14] M. H. A. Begum, M. M. Hossain, M. A. Gafur, A. N. M. H. Kabir, N. I. Tanvir *et al*., *SN Appl. Sci*. **1**, 1 (2019), https://doi.org/10.1007/s42452-019-1111-2

[15] A. Berkkan, E. Kondolot Solak and G. Asman, *ChemistrySelect*, **6**, 5678 (2021), https://doi.org/10.1002/slct.202100917

[16] A. Ounkaew, P. Kasemsiri, K. Jetsrisuparb, H. Uyama, Y. I. Hsu *et al.*, *Carbohyd. Polym.*, **248**, 116767 (2020), https://doi.org/10.1016/j.carbpol.2020.116767
[17] Q. Liang, W. Pan and Q. Gao, *Int. J. Biol. Macromol.*, **190**, 601 (2021), https://doi.org/10.1016/j.ijbiomac.2021.09.015
[18] E. Sharmin, M. T. Kafyah, A. A. Alzaydi, A. A. Fatani, F. A. Hazazzi *et al.*, *Int. J. Biol. Macromol.*, **163**, 2236 (2020), https://doi.org/10.1016/j.ijbiomac.2020.09.044
[19] M. Lopez-Silva, L. A. Bello-Perez, E. Agama-Acevedo and J. Alvarez-Ramirez, *Food Hydrocoll.*, **97**, 105212 (2019), https://doi.org/10.1016/j.foodhyd.2019.105212
[20] P. Suwannaporn, S. Pitiphunpong and S. Champangern, *Starch/Staerke*, **59**, 171 (2007), https://doi.org/10.1002/star.200600565
[21] B. K. Baik and M. R. Lee, *Cereal Chem.*, **80**, 304 (2003), https://doi.org/10.1094/CCHEM.2003.80.3.304
[22] C. Yu, W. Lin, J. Jiang, Z. Jing, P. Hong *et al.*, *RSC Adv.*, **9**, 37759 (2019), https://doi.org/10.1039/c9ra06848a
[23] S. Wang, R. Castro, X. An, C. Song, Y. Luo *et al.*, *J. Mater. Chem.*, **22**, 23357 (2012), https://doi.org/10.1039/c2jm34249a
[24] P. P. Patil, J. V. Meshram, R. A. Bohara, S. G. Nanaware and S. H. Pawar, *New J. Chem.*, **42**, 14620 (2018), https://doi.org/10.1039/C8NJ01675E
[25] I. Govindaraju, G. Y. Zhuo, I. Chakraborty, S. K. Melanthota, S. S. Mal *et al.*, *Food Hydrocoll.*, **122**, 107093 (2022), https://doi.org/10.1016/j.foodhyd.2021.107093
[26] N. A. Azahari, N. Othman and H. Ismail, *J. Phys. Sci.*, **22**, 15 (2011), https://doi.org/https://jps.usm.my/wp-content/uploads/2014/10/22.2.2.pdf
[27] A. Sarkar, D. R. Biswas, S. C. Datta, B. S. Dwivedi, R. Bhattacharyya *et al.*, *Carbohyd. Polym.*, **259**, 117679 (2021), https://doi.org/10.1016/j.carbpol.2021.117679
[28] J. Waterschoot, S. V. Gomand, E. Fierens and J. A. Delcour, *Starch/Staerke*, **67**, 14 (2015), https://doi.org/10.1002/star.201300238
[29] M. Mozafari, J. Moztarzadeh, N. Alhosseini, S. Asgari, M. Dodel *et al.*, *Int. J. Nanomed.*, **7**, 25 (2012), https://doi.org/10.2147/IJN.S25376
[30] A. Kharazmi, N. Faraji, R. M. Hussin, E. Saion, W. M. M. Yunus *et al.*, *Beilstein J. Nanotechnol.*, **6**, 529 (2015), https://doi.org/10.3762/bjnano.6.55
[31] N. V. Bhat, M. M. Nate, M. B. Kurup, V. A. Bambole and S. Sabharwal, *Nucl. Instrum. Methods Phys. Res. B*, **237**, 585 (2005), https://doi.org/10.1016/j.nimb.2005.04.058
[32] A. H. D. Abdullah, S. Chalimah, I. Primadona and M. H. G. Hanantyo, *IOP Conf. Ser. Earth Environ. Sci.*, **160**, 012003 (2018), https://doi.org/10.1088/1755-1315/160/1/012003
[33] C. Anchondo-Trejo, J. A. Loya-Carrasco, T. Galicia-García, I. Estrada-Moreno, M. Mendoza-Duarte *et al.*, *Molecules*, **26**, 54 (2020), https://doi.org/10.3390/molecules26010054
[34] M. G. Lomelí-Ramírez, A. J. Barrios-Guzmán, S. García-Enriquez, J. de Jesús Rivera-Prado and R. Manríquez-González, *BioResources*, **9**, 2960 (2014), https://doi.org/10.15376/biores.9.2.2960-2974
[35] P. V. Kowsik and N. Mazumder, *Microsc. Res. Tech.*, **81**, 1533 (2018), https://doi.org/10.1002/jemt.23160
[36] A. Das, R. Uppaluri and C. Das, *Int. J. Biol. Macromol.*, **131**, 998 (2019), https://doi.org/10.1016/j.ijbiomac.2019.03.160
[37] H. Adeli, M. T. Khorasani and M. Parvazinia, *Int. J. Biol. Macromol.*, **122**, 238 (2019), https://doi.org/10.1016/j.ijbiomac.2018.10.115
[38] F. Mirab, M. Eslamian and R. Bagheri, *Biomed. Phys. Eng. Express*, **4**, 055021 (2018), https://doi.org/10.1088/2057-1976/aad74a
[39] S. Ceylan, D. Göktürk, D. Demir, M. Damla Özdemir and N. Bölgen, *Int. J. Polym. Mater. Polym. Biomater.*, **67**, 855 (2018), https://doi.org/10.1080/00914037.2017.1383254
[40] K. Kemashalini, B. D. R. Prasantha and K. A. K. L. Chandrasiri, *Adv. Food Sci. Eng.*, **2**, 115 (2018), https://doi.org/10.22606/afse.2018.24003
[41] R. Ray, S. Narayan Das and A. Das, *Mater. Today Proc.*, **41**, 376 (2019), https://doi.org/10.1016/j.matpr.2020.09.564
[42] E. A. Bursali, S. Coskun, M. Kizil and M. Yurdakoc, *Carbohyd. Polym.*, **83**, 1377 (2011), https://doi.org/10.1016/j.carbpol.2010.09.056
[43] P. Di Martino, *AIMS Microbiol.*, **4**, 563 (2018), https://doi.org/10.3934/microbiol.2018.3.563
[44] K. Vengadesan and S. V. L. Narayana, *Protein Sci.*, **20**, 759 (2011), https://doi.org/10.1002/pro.613
[45] G. Sharma, S. Sharma, P. Sharma, D. Chandola, S. Dang *et al.*, *J. Appl. Microbiol.*, **121**, 309 (2016), https://doi.org/10.1111/jam.13078
[46] J. L. Lister and A. R. Horswill, *Front. Cell. Infect. Microbiol.*, **4**, 178 (2014), https://doi.org/10.3389/fcimb.2014.00178
[47] ASTM F 756-00, Standard Practice for Assessment of Hemolytic Properties of Materials, 2017, https://doi.org/10.1520/F0756-13